



NMR (^{13}C , ^{17}O), IR and Raman Studies of Poly-nuclear Carbonyls Transition Metal Carbonyls : A DFT Application

M.L.SEHGAL¹, AMIT AGGARWAL² and MD. IRSHAD AHMAD^{3*}

¹Department of Chemistry, D.A.V. College, Jalandhar-144008, India.

²Department of Natural Sciences, LaGuardia Community College of The City University of the New York, 31-10 Thomson Avenue, Long island City, 11101, New York, USA.

³Department of Biochemistry, Aligarh Muslim University, Aligarh, 202002, Uttar Pradesh, India.

*Corresponding author E-mail: irshadahmad.bio@gmail.com

<http://dx.doi.org/10.13005/ojc/330201>

(Received: March 25, 2017; Accepted: April 12, 2017)

ABSTRACT

DFT implemented in ADF 2012.01 was used to know about the relative spatial displacements of three/four metals and the surrounding 12 terminal and bridging CO groups in 5 poly-nuclear carbonyls: $[\text{M}_3(\text{CO})_{12}]$, (M=Ru, Os), $[\text{Ir}_3(\text{CO})_{12}]$, $[\text{Fe}_3(\text{CO})_{12}]$ and $[\text{Rh}_4(\text{CO})_{12}]$. After optimization, the software was first run using the "NMR Program" with Single Point, Default, None, Collinear, Nosym using TZP or TZ2P Basis sets leaving Unrestricted command blank to obtain the Shielding Constants (σ_M , $\sigma^{13}\text{C}$, $\sigma^{17}\text{O}$), the Chemical Shifts (δ_M , $\delta^{13}\text{C}$, $\delta^{17}\text{O}$), 2 diamagnetic and 4 paramagnetic contributing terms in the σ values of constituents. The k and j values of constituents were obtained from the same program by using a new Input File. There after, the software was run with Frequencies and Raman full to obtain frequencies of the normal modes of all the (3n-6) Fundamental vibration bands of the carbonyls. All the metals in the above named first three carbonyls were spatially equivalent while in the latter two carbonyls, all the metals were not equivalent. But no where, the two metals or any two COs were found to be magnetically equivalent. Excepting $\text{Ir}_4(\text{CO})_{12}$ where all the 12 CO groups were spatially equivalent, in other four carbonyls, CO groups were found to be two or more types spatially. The first metal and the responding spatially equivalent other metal/s possessed same k and j values. For CO groups attached to one metal and spatially equivalent CO groups attached to other spatially equivalent metal/s, k and j values of ^{13}C nuclei possessed the same values. A perturbing metal and spatially equivalent responding metal/s along with spatially equivalent CO groups had same k and j values respectively. The study was important in four ways. Firstly, using these parameters, we could calculate quite a more number of parameters such as Effective Spin Hamiltonian (H^{Spin}) of the metals and ^{13}C nuclei, Coordination Shifts ($\Delta_\delta^{13}\text{C}$, $\Delta_\delta^{17}\text{O}$), atomic electron valence density (integrated)/ L value of ^{17}O and charges on both the ^{17}O and metals along with spatial displacements/stereochemical equivalences of constituents. Secondly, we could correlate these NMR parameters with their reported IR/Raman results which lent credence to their II-acid character. Thirdly, we classified their fundamental vibration bands types into four types. Fourthly, we could arrive at some optimization and thermal parameters of carbonyls.

Keywords: Chemical Shift, Shielding Tensor, Paramagnetic Tensor, Effective Spin Hamiltonian, Magnetic Equivalence

INTRODUCTION

We had successfully applied DFT to study NMR parameters such as: Shielding Constants (σ_M , σ^{13C} , σ^{17O}), Chemical Shifts (δ_M , δ^{13C} , δ^{17O}), two diamagnetic and four paramagnetic contributing terms in the σ values of constituents, the k and j values, Effective Spin Hamiltonian (H^{Spin}) of the metals and 13C nuclei and Coordination Shifts (Δ_δ^{13C} , Δ_δ^{17O}) for the 11 mononuclear¹⁻³ and 9 binuclear⁴ carbonyls of the 1st, 2nd and 3rd transition metals. Of course, Schreckenbach *et al.*, had, first of all, applied DFT to 13C and 17O NMR spectra to a few mono-nuclear transition metal carbonyls of the metals like $M=Cr^{5,6}$, Mo^6 , $W^{5,6}$, $Fe^{5,7}$, $Ru^{5,7}$, $Os^{5,7}$ to obtain their δ , σ and bond dissociation energies.

Carbonyls such as $[M_2(CO)_n]$ ($M=V$, Nb ; $n=10-12$)¹⁵⁻¹⁷ which did not obey "The 18 Electron Rule" were not taken up because of their doubtful stability.

But unlike the vast variety of NMR parameters of 20 mono- and bi-nuclear⁸⁻¹⁴ carbonyls studied by our group of workers^{1,4}, only a little had been reported on NMR studies by computational methods for poly-nuclear¹⁸⁻²² carbonyls as follows:

Variable temperature 13C NMR spectra of the carbonyls $M_3(CO)_{12}$ ($M = Fe, Ru, \text{ and } Os$) and other related compounds¹⁸ were reported. At least three CO scrambling processes had been shown to operate in these system. Mössbauer spectroscopic studies of iron carbonyls adsorbed on $\gamma-Al_2O_3$ and SiO_2 were carried out by Iwai *et al.*,¹⁹ while 1H NMR and IR spectra of ruthenium and osmium carbonyl clusters incorporating stannylene and stannyl ligands were studied by Shariff E. Kabir and his co-workers²⁰. Fang²¹ submitted his thesis (2012) on, "Studies of iridium carbonyl cluster complexes,". He prepared five polynuclear iridium-germanium mixed carbonyl-phenyl complexes and studied their X-ray structures and 1H NMR by applying DFT. The same properties were studied by Yuwei Kan²² in his thesis (2013) entitled, "New ruthenium and osmium carbonyl cluster complexes with main group bridging ligands having unusual structures and bonding".

The present study includes 5 poly-nuclear carbonyls of transition metals in their zero oxidation

states as: $[M_3(CO)_{12}]$, ($M=Ru, Os$), $[Ir_4(CO)_{12}]$, $[Fe_3(CO)_{12}]$ and $[Rh_4(CO)_{12}]$. The first 3 carbonyls contained only terminal CO groups while the other two possessed both terminal and bridging CO groups. All these carbonyls obeyed "The 18 Electron Rule". The software did not work in $[Co_3(CO)_{12}]$.

This manuscript was subdivided as follows:

- (i) It would include structures of five polynuclear carbonyls and the explanation in the difference their NMR parameters, Spatial and Magnetic Equivalences of the three/ four metals and the 12 CO groups on the basis of their structures.
- (ii) Then we would take up the calculation of Effective Spin Hamiltonian (H^{Spin}) of the metals and the 13C nuclei, the division of (3n-6) fundamental vibration bands into Vibration Symmetry Classes and their IR/ Raman activities.
- (iii) Lastly, there would be a discussion on the corroboration of NMR results with the reported IR and Raman results, the higher AEVD {Atomic Electron Valence Density (integrated)/ L} and the higher negative charge on 17O of CO of metal carbonyl than 17O of CO(g) and slight increase in positive charge on the metals of the five carbonyls.

Need of the study

The following three points necessitated the use of a software for this study.

- (I) Computational Chemistry had, hardly, been used in ascertaining the pi-acid character of the poly-nuclear carbonyls by NMR technique though such studies were reported for mono-nuclear¹ and bi-nuclear carbonyls⁴.
- (II) A range of symmetries, i.e. D_{3h} to C_{2v} existing in equilibrium was reported for $[Fe_3(CO)_{12}]$ by Cotton and Hunter²³. But X-rays and Moss Bauer techniques have predicted only C_{2v} symmetry for it. We would try to ascertain whether our NMR study could give a fillip to its Mossbauer studies or not. It was the Mossbauer technique which first of all confirmed C_{2v} structure of $[Fe_3(CO)_{12}]$ with two quadrupole doublets having similar isomer shifts but different

quadrupolar coupling constants (1.13 and 0.13 mm s⁻¹)^{23,24}.

- (III) There could occur errors in the values of the experimentally determined vibration frequencies of bands as they were affected by coupling with neighboring group vibrations. Also, ADF software could become a better choice since it calculates Raman intensities from the polarizabilities of Raman bands.

Importance of the study

- (a) The values of thermal parameters like zero-point energy, moments of inertia, entropy, internal energy and heat capacity at constant volume which will be reported for the polynuclear transition metal carbonyls for the first time may prove helpful to the future scientists in studying their other physical properties.
- (b) Efforts will be made to exploit this technique to study Metal to Ligand Transfer (MLCT) phenomenon for macro cyclic bis- and tris- complexes of 2, 2-bipyridine and 1,10-phenanthroline ligands with transition metal ions.

Materials, Method and Experimental details¹⁻³

ADF software was installed on Windows XP platform as "ADF jobs". A new directory was created using "File menu" of ADF jobs. After optimization of the metal carbonyl, different commands were filled into the software to obtain a number NMR and IR/Raman parameter^{1,4} such as δ, σ, k, j for M, ¹³C and ¹⁷O of carbonyls, values of two diamagnetic and four paramagnetic contributing terms which constitute σ values of these constituents along with atomic electron valence density (integrated) / L value of ¹⁷O and charges on the ¹⁷O and metals. Diamagnetic terms were named as: {a} diamagnetic core and {b} diamagnetic valence tensor

while the four paramagnetic terms were called: {c} paramagnetic (b[^]) tensor, {d} paramagnetic (u[^]) tensor, {e} paramagnetic(s[^]) tensor and {f} paramagnetic gauge tensors. Four more parameters namely Coordination Shifts ($\Delta_{\delta}^{13C}, \Delta_{\delta}^{17O}$), Effective Spin Hamiltonian (H[^]) of M and ¹³C of carbonyls, atomic electron valence density (integrated) / L value of oxygen and charges on both the oxygen and metal atoms to elucidate the relative spatial arrangements of three /four metal ions and the 12 bridging and terminal CO groups was developed.

We obtained IR/ Raman parameters by giving different commands¹⁻³ to the software and corroborated them with NMR parameters to ascertain the π - acid nature of carbonyls.

RESULTS

Tables:1, 2 gave optimization and thermal parameters respectively. Tables: 3-5 represented σ_M, σ^{13C} and σ^{17O} values and their 6 contributing terms respectively. Table:6 gave total values of diamagnetic and paramagnetic terms. Tables:7 contained $\sigma^{13C}, \delta^{13C}, \Delta \delta^{13C}, \sigma^{17O}, \delta^{17O}, \Delta \delta^{17O}$. Table:8 contained types of metals and Charge on each. Table:9 contained σ^{17O} , Charges and Atomic Electron Valence Density (integrated) / L Value on oxygen. Table:10 gave ADF numbers and σ^{13C} of ¹³C nuclei bonded to various metals. Table:11 gave Spatial Classification of Metals and COs. Table:12 gave k, j and H^{spin} values of species. Table:13 represented fundamental vibration bands and their classification in terms of their IR/Raman activities. Table:14 represented Total Coordination Shifts and ν_{CO} (cm⁻¹) of [M₃(CO)₁₂] (M= Ru, Os)

Figures:1-5 of the carbonyls would give ADF numbers which were mentioned in the tables

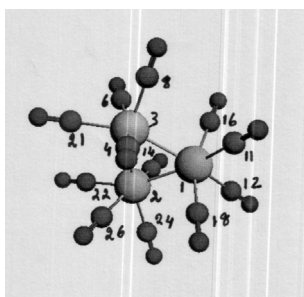


Fig.1: D₃ stereochemistry of Ru₃(CO)₁₂

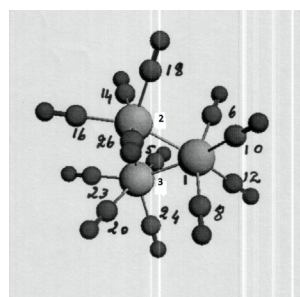


Fig. 2: D₃ stereochemistry of Os₃(CO)₁₂

- (b) The relation between (σ) and (δ) for carbon was given as follows:
 $\delta^{13}\text{C} = 181.1 - \sigma^{13}\text{C}$... (2)
- (c) δM and $\delta^{17}\text{O}$ were numerically equal to σM and $\sigma^{17}\text{O}$ but had reverse signs.
 $\sigma\text{M} = -\delta\text{M}$
 $\sigma^{17}\text{O} = -\delta^{17}\text{O}$... (3)
- (d) The parameters $\{\delta^{13}\text{C}, \delta^{17}\text{O}, \sigma^{13}\text{C}, \sigma^{17}\text{O}\}$ were, then, compared with their Coordination Shifts $\{\Delta_{\delta}^{13}\text{C}, \Delta_{\delta}^{17}\text{O}\}$ by using the following relations:
 $\Delta_{\delta}^{13}\text{C} = \sigma^{13}\text{C}(\text{MCO}) - (-34.44)$... (4)
 $\Delta_{\delta}^{17}\text{O} = \sigma^{17}\text{O}(\text{MCO}) - (-129.53)$... (5)
- (e) The Total Coordination Shifts $\{\Delta_{\delta}^{13}\text{C}_T, \Delta_{\delta}^{17}\text{O}_T\}$ was calculated as follows:
 $\Delta_{\delta}^{13}\text{C}_T = [\{\sigma^{13}\text{C}(\text{MCO}) - (-34.44)\} \times \text{Number of spatially equivalent } ^{13}\text{C} \text{ nuclei of 1}^{\text{st}} \text{ type}] + [\{\sigma^{17}\text{O}(\text{MCO}) - (-129.53)\} \times \text{Number of spatially equivalent } ^{17}\text{O} \text{ nuclei of 1}^{\text{st}} \text{ type}] + \dots$ so on ... (6)
- (f) For isolated carbon, $\sigma_{\text{reference}} = -181.1$ ppm. So, $\sigma_{\text{reference}}$ for carbon of CO (g) and the carbon of metal carbonyls should be different because the electron densities on the isolated carbon, the carbon present in CO (g) and the carbon of a metal carbonyl would be different and the terms called Coordination shifts (Δ_{δ}), analogous to Chemical shifts, were calculated with reference values.
- (g) The π -acid ligand CO should donate electron density to the metal via dative σ bond ($\text{OC} \rightarrow \text{M}$) to increase electron density

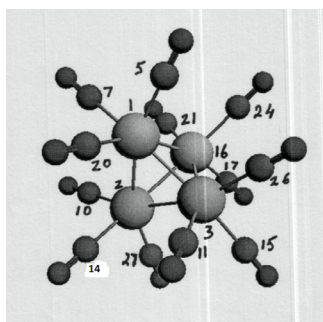
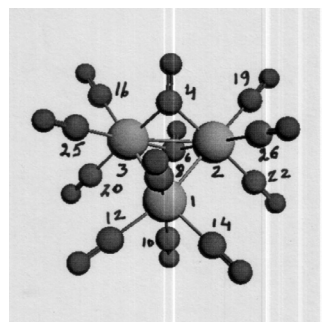
Fig. 3: T_d stereochemistry of $\text{Ir}_4(\text{CO})_{12}$ Fig. 4: C_{2v} stereochemistry of $\text{Fe}_3(\text{CO})_{12}$

Table 1: Optimization Parameters of Poly-nuclear Carbonyls

Carbonyl Dipole moment (D)	Point group	Total bonding Energy*	Total Energy: Xc** (LDA)** k J mol ⁻¹	Nucleus	I
$\text{Ru}_3(\text{CO})_{12}$ (0.04)	D_{3h}	-19692.31	-1389956.20 (-1328606.25, -61349.95)	¹⁰¹ Ru	2.5
$\text{Os}_3(\text{CO})_{12}$ (0.05)	-do-	-20795.51	-2854950.18 (-2764119.34, -90830.85)	¹⁸⁷ Os	1.5
$\text{Ir}_4(\text{CO})_{12}$ (0.03)	T_d	-21464.98	-3747674.96 (-3634920.32, -112754.65)	¹⁹¹ Ir	1.5
$\text{Fe}_3(\text{CO})_{12}$ (2.97)	C_{2v}	-19863.97	-809510.65 (-763180.82, -46329.83)	57Fe	0.5
$\text{Rh}_4(\text{CO})_{12}$ (2.917)	C_{3v}	-19891.27	-1772474.41 (-1699114.86, -73359.55)	103 Rh	0.5

*Bonding energy is computed as an energy difference between molecule and fragments**Xc contains LDA and GGA Components; both contain *Exchange* and *Correlation* parts; GGA is zero in all the three carbonyls

on metal. But due to a strong Π back donation from the filled d orbitals of metal to energetically favorable and geometrically suitable vacant Π^* molecular orbitals of CO ($OC \rightarrow M$), electron density should be reduced on the metal to cause an increase in the electron density on CO. As σ of a nucleus was directly related to electron density, any change in the value of its σ should serve as an indicator to the change in electron density. Hence, if CO was to act as a back acceptor, $\sigma^{13}C$ of metal carbonyls should become more than $\sigma^{13}C$ of CO (g). But according to vibration (IR/Raman) spectroscopy, the Π back donation of CO would cause a decrease in ν_{CO} in metal carbonyls with respect to pure CO(g) ($\nu_{CO} = 2143 \text{ cm}^{-1}$)²⁶.

(h) Some of this increased electron density on

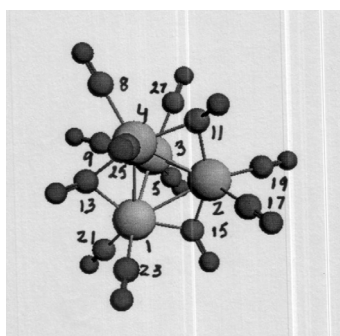


Fig. 5: C_{3v} stereochemistry of $Rh_4(CO)_{12}$

carbon was also transmitted to oxygen of CO group to make their $\sigma^{17}O$ also more than that that in free CO.

- (i) Relative spatial displacements of constituting species were reaffirmed from shielding constants of the M, C and O $\{\sigma^M, \sigma^{13}C(MCO), \sigma^{17}O(MCO)\}$ simply by the fact that the spatially equivalent species should have same values of shielding constants along with their constituting two diamagnetic and four paramagnetic terms respectively.

Structures, NMR and IR/ Raman Parameters of poly-nuclear carbonyls

Their discussion was subdivided into nine headings (4.2.1- 4.2.9) as follows:

Trends in NMR parameters of 5 poly-nuclear carbonyls

- (1) Even if the 3 or 4 metals were found to be spatially equivalent, their CO groups might possess different NMR parameters like $\sigma^{13}C$, $\sigma^{13}O$, $\delta^{13}C$, $\delta^{13}O$.
- (2) Depending upon the geometry, even the COs attached to the same metal might differ spatially to give more than one value of $\sigma^{13}C$, $\delta^{13}C$ and $\sigma^{17}O$, $\delta^{17}O$.

Of course, the spatially equivalent species were always expected to have the same values of the 2 diamagnetic and 4 paramagnetic terms which contribute to the

Table. 2: Thermal Parameters of Poly-nuclear Carbonyls at 298 K

Carbonyl	Zero Point Energy (eV)	Some Thermal Parameters											
		Entropy ($\text{cal mol}^{-1}\text{K}^{-1}$)				Internal Energy (Kcal mol^{-1})				Constant Volume Capacity ($\text{Kcal mol}^{-1}\text{K}^{-1}$)			
		Trans.	Rot.	Vib.	Total	Trans.	Rot.	Vib.	Total	Trans.	Rot.	Vib.	Total
$Ru_3(CO)_{12}$	2.169	45.259	32.40	64.64	142.313	-do-	-do-	60.912	62.689	-do-	-do-	62.07	68.028
$Os_3(CO)_{12}$	1.904	46.306	32.75	69.43	148.491	-do-	-do-	63.229	65.006	-do-	-do-	66.76	72.721
$Ir_4(CO)_{12}$	2.211	46.887	32.03	81.34	160.259	-do-	-do-	64.51	66.29	-do-	-do-	74.34	80.299
$Fe_3(CO)_{12}$	2.229	44.538	34.11	72.96	51.628	0.889	0.889	63.383	65.161	2.981	2.981	68.82	74.787
$Rh_4(CO)_{12}$	2.211	45.714	34.19	85.40	165.300	-do-	-do-	64.73	66.511	-do-	-do-	77.60	83.566

- total values of their σ parameters respectively (Tables: 3-6).
- (3) The same inference was drawn from the charges on the metal ions where the spatially equivalent metals possessed the same charges while the spatially different metals possessed different charges (Table: 8).
- (4) $[M_3(CO)_{12}]$ (M= Ru, Os) contained of two types of terminal (T-1; T-2) COs; six of each type (Table-10) with two sets of $\sigma^{13}C$, $\sigma^{17}O$ and $\delta^{13}C$, $\delta^{17}O$ values.
- (5) $[Ir_4(CO)_{12}]$ possessed 12 equivalents terminal (T) COs (Table-10) with the same set of values for $\sigma^{13}C$, $\sigma^{17}O$, $\delta^{13}C$, $\delta^{17}O$ parameters respectively.
- (6) $[Fe_3(CO)_{12}]$ and $[Rh_4(CO)_{12}]$ possessed both terminal and bridging COs; the terminal showed back-accepting property while bridged COs like carbonyl group, did not act as a back acceptors. So the electron density on bridging and terminal COs would differ largely to give different $\sigma^{13}C$ and $\delta^{13}C$ values.
- (7) Further, bridging COs might be bonded to two different sets of Fe (0) or R h (0) to show two or more types of $\sigma^{13}C$, $\sigma^{17}O$, $\delta^{13}C$, $\delta^{17}O$

Table 3: σ M, Diamagnetic and Paramagnetic Contributions [p pm]

Carbonyl ^a	σ M	Diamagnetic Contributions		Paramagnetic Contributions			
		{a}	{b}	{c}	{d}	{e}	{f}
Ru ₃ (CO) ₁₂ (1)	Ru(1,2,3) -1742.1	4161.944	,96.31	540.901,-6803.485,	265.34,	-3.066	
Os ₃ (CO) ₁₂ (2)	Os (1,2,3) 2823.1	8814.709	,238.77	662.065,-6855.089,	-32.966,	-4.426	
Ir ₄ (CO) ₁₂ (3)	Ir(1,2,3,16)1886.2	8956.268,	264.36	557.80,-7660.153,	-231.292,	-0.782	
Fe ₃ (CO) ₁₂ (4)	Fe6(1) -4798.7	1907.269,	127.66	-217.75,-7644.23,	1041.906	-13.58	
	Fe7(2,3)-4293.4	1907.240	,128.43	-241.245,-6873.934,	797.975,	-8.813	
Rh ₄ (CO) ₁₂ (5)	Rh7(1,2,4)-753.8	4274.142,	122.34	-654.353,-5266.00,	775.955,	-6.072	
	Rh6(3) -630.93	4274.135,	118.46	-666.97 ,	-5493.796,	1145.84	-8.595

Table 4: $\sigma^{13}C$, Diamagnetic and Paramagnetic Contributions [p pm]

Carbonyl ^a	$\sigma^{13}C$	Diamagnetic Contributions		Para magnetic Contributions			
		{a}	{b}	{c}	{d}	{e}	{f}
Ru ₃ (CO) ₁₂ (1)	C (4,6,16,18,22,24)-67.23	199.233,	49.493	2.003,	-350.460,	28.805,	3.698
	C (8,11,12,14,21,26)-31.2	199.233,	48.692	-0.935,-307.488,	28.243	,1.061	
OS ₃ (CO) ₁₂ (2)	C (5,6,8,18,20,26)-23.63	199.232,	48.935	-0.117 ,	-304.919,	32.923,	0.312
	C (10,12,14,16,23,24)-53.9	199.233,	50.241	0.742,-337.539,	29.955,	3.439	
Ir ₄ (CO) ₁₂ (3)	C(5,7,10,11,14,15,17,20,	199.232,	51.388	0.284 ,	-281.927,	35.577 ,	0.846
	21,24,26,27) 5.41						
Fe ₃ (CO) ₁₂ (4)	C (4,6)-120.66	199.223,	45.460	3.269,	-424.572,	66.024 ,	-10.068
	C (8,10) -13.01	199.227,	49.056	-0.659 ,	-291.828,	31.829,	-0.635
	C (12,14)-39.11	199.226,	49.308	1.508,	-319.762,	28.437,	2.177
	C (16,19,20,22) -24.0	199.227,	48.983	0.102,	-303.386,	30.303,	0.758
Rh ₄ (CO) ₁₂ (5)	C (25,26) -1.89	199.225,	49.238	-1.460 ,	-275.199,	24.531,	1.778
	C (5,9,27) 2.81	199.227,	49.993	-0.289,	-273.247,	26.856,	0.267
	C (8,19,21) -0.55	199.227,	51.445	1.083 ,	-278.439,	23.921,	2.216
	C (11,13,15)-77.52	199.230,	43.277	0.541,	-362.892,	44.744,	-2.420
	C (17,23,25) -4.99	199.226,	51.082	0.174,	-279.547,	22.862 ,	1.212

a. ADF Numbers in parentheses [Figs: 1-5]

Table 5. $\sigma^{17}\text{O}$, Diamagnetic and Paramagnetic Contributions [p pm]

Carbonyl (Fig. No.)	$\sigma^{17}\text{O}$	Diamagnetic Contributions		Paramagnetic Contributions			
		{a}	{b}	{c}	{d}	{e}	{f}
Ru ₃ (CO) ₁₂ (1)	O (5,7,17,19,23,25)-192.82	269.472	129.954	1.788	-539.118	-53.474	-1.439
	O (9,10,13,15,20,27)-115.5	269.472	129.314	-0.397	-461.428	-51.517	-0.924
Os ₃ (CO) ₁₂ (2)	O (4,7,9,19,21,27)-94.67	269.472	129.012	-0.104	-444.782	-46.704	-1.578
	O (11,13,15,17,22,25)-155.0	269.472	129.982	1.115	-509.706	-43.737	-2.143
Ir ₄ (CO) ₁₂ (3)	O(4,6,8,9,12,13,18,19,22, 23,25,28) -41.57	269.472	130.284	0.341	-396.061	-44.261	-1.336
	O (5,7) -468.88	269.467	133.908	0.458	-732.984	-135.456	-4.27
Fe ₃ (CO) ₁₂ (4)	O (9,11) -59.35	269.470	129.938	-0.191	-410.922	-45.114	-2.532
	O (13,15) -117.54	269.470	129.878	1.129	-480.661	-35.301	-2.051
	O (17,18,21,23) -82.34	269.470	130.174	0.276	-434.934	-45.182	-2.147
	O (24,27) -38.23	269.468	130.003	-0.639	-396.341	-39.915	-0.803
	O (6,10,28) -48.23	269.469	129.853	-0.150	-398.640	-46.658	-2.097
Rh ₄ (CO) ₁₂ (5)	O (7,20,22) -49.40	269.470	129.851	0.795	-412.121	-37.601	0.205
	O (12,14,16) -337.92	269.468	135.290	-0.471	-578.495	-158.855	-4.86
	O (18,24,26) -57.92	269.469	130.088	0.064	-409.253	-47.276	-1.014

Table 6: Total Diamagnetic, Paramagnetic contributions in σ^{M} , $\sigma^{13}\text{C}$ and $\sigma^{17}\text{O}$ [p pm]

Carbonyl (Fig. No.)	ADF Nos. of M	Diamag. Contrib.	Paramag. Contrib.	ADF Nos. of C	Diamag. Contrib.	Paramag. Contrib.	ADF Nos. of O	Diamag. Contrib.	Paramag. Contrib.
Ru ₃ (CO) ₁₂ (1)	Ru(1,2,3)	4258.26	-6000.31	(4,6,16, 18,22,24)	248.727	-316	(5,7,17, 19,23,25)	399.43	-592.243
				(8,11,12, 14,21,26)	247.926	-279.1	(9,10,13, 15,20,27)	398.79	-514.266
				(5,6,8, 18,20,26)	248.168	-271.8	(4,7,9,19, 21,21,27)	398.49	-493.169
Os ₃ (CO) ₁₂ (2)	Os (1,2,3)	9053.48	-6230.35	(10,12,14, 16,23,24)	249.474	-303.4	(1113,15, 17,22,25)	399.45	-554.471
				(5,7,10, 11,14,15, 17,20,21, 24,26,27)	250.62	-245.2	(4,6,8, 9,12,13, 18,19,22, 23,25,28)	399.76	-441.329
				(4,6)	244.683	-365.3	(5,7)	403.38	-872.25
Fe ₃ (CO) ₁₂ (4)	Fe6(1) Fe7(2,3)	2034.93 2035.67	-6833.66 -6326.02	(8,10)	248.282	-261.3	(9,11)	399.41	-458.758
				(12,14)	248.533	-287.6	(13,15)	399.35	-516.883
				(16,19, 20,22)	248.209	-272.2	(17,18, 21,23)	399.64	-481.987
				(25,26)	248.463	-250.4	(24,27)	399.47	-437.698
				(5,9,27)	249.219	-246.4	(6,10,28)	399.32	-447.545
Rh ₄ (CO) ₁₂ (5)	Rh7(1,2,4) Rh6(3)	4396.48 4392.59	-5150.43 -5023.52	(8,19,21)	250.673	-251.2	(7,20,22)	399.32	-448.722
				(11,13,15)	242.507	-320	(12,14,16)	404.78	-742.675
				(17,23,25)	250.308	-255.3	(18,24,26)	399.56	-457.478

a. ADF Numbers in parentheses [Figs: 1-5]

in addition to one or more types of σ M and δ M for the three/four metals which enabled us to confirm the relative spatial displacements of the three/four metals and the 12 COs

around them simply from their σ and δ values. The spatially equivalent species were also expected to have the same values of two diamagnetic and four paramagnetic terms

Table 7: σ ^{13}C , δ ^{13}C , Δ δ ^{13}C , σ ^{17}O , δ ^{17}O , and Δ δ ^{17}O Values [p pm] of Carbonyls

Carbonyl ^a	ADF No. of C	δ ^{13}C [2]*	σ ^{13}C	Δ δ ^{13}C _T [4]**	ADF No. of O	δ ^{17}O [3]*	σ ^{17}O	Δ δ ^{17}O _T [5]**
Ru ₃ (CO) ₁₂ (1)	(4,6,16, 18,22,24)	248.32	-67.23	-196.74	(5,7,17, 19,23,25)	192.8	-192.8	-379.62
	(8,11,12, 14,21,26)	212.29	-31.2	19.44	(9,10,13, 15,20,27)	115.5	-115.5	84.18
	----	----	----	[-177.3]	---	---	---	[-295.44]
Os ₃ (CO) ₁₂ (2)	(5,6,8, 18,20,26)	204.735	-23.63	64.86	(4,7,9,19, 21,21,27)	94.7	-94.7	208.98
	(10,12,14, 16,23,24)	235.03	-53.9	-116.76	(11,13,15, 17,22,25)	155	-155	-152.82
	---	---	---	[-51.9]	---	---	---	[56.16]
Ir ₄ (CO) ₁₂ (3)	(5,7,10, 11,14,15, 17,20,21, 24,26,27)	175.7	-5.41	[478.2]	(4,6,8, 9,12,13, 18,19,22, 23,25,28)	41.57	-41.57	[1055.52]
	Fe ₃ (CO) ₁₂ (4)	(4,6)	301.77	-120.66	-172.44	(5,7)	468.88	-468.88
Fe ₃ (CO) ₁₂ (4)	(8,10)	194.11	-13.01	42.86	(9,11)	59.35	-59.35	140.36
	(12,14)	220.21	-39.11	-9.34	(13,15)	117.54	-117.54	23.98
	(16,19, 20,22)	205.11	-24	41.76	(17,18, 21,23)	82.34	-82.34	188.76
	(25,26)	182.99	-1.89	65.1	(24,27)	38.23	-38.23	182.6
	----	----	----	[-32.06]	---	---	---	[-143.0]
Rh ₄ (CO) ₁₂ (5)	(5,9,27)	178.28	2.81	111.75	(6,10,28)	48.23	-48.23	243.9
	(8,19,21)	181.65	9-0.55	101.67	(7,20,22)	49.4	-49.4	240.39
	(11,13,15)	258.62	-77.52	-129.24	(12,14,16)	337.92	-337.92	-625.17
	(17,23,25)	186.09	-4.99	88.35	(18,24,26)	57.92	-57.92	214.83
	---	---	----	[172.53]	---	---	---	[73.95]

a. ADF Numbers in parentheses [Figs: 1-5] *Apply relations: 2, 3. ** Calculate by relations 4 and 5

Table 8: Charges and Types of Metal Ions

Carbonyl	ADF numbers of Metal Ions	Charges on Metal Ions	Types of Metal Ions
Ru ₃ (CO) ₁₂	Ru(1,2,3)	0.2711	1
Os ₃ (CO) ₁₂	Os (1,2,3)	0.2758	1
Ir ₄ (CO) ₁₂	Ir (1,2,3,16)	0.1807	1
Fe ₃ (CO) ₁₂	Fe ⁶ (1)	0.0537	2
	Fe ⁷ (2,3)	0.1508	
Rh ₄ (CO) ₁₂	Rh ⁷ (1,2,4)	0.2994	2
	Rh ⁶ (3)	0.4011	

- which contribute to the total values of their σ parameters.
- (8) $[\text{Fe}_3(\text{CO})_{12}]$ and $[\text{Rh}_4(\text{CO})_{12}]$ possessed two types of Fe (0) and Rh (0) respectively. The two Fe (0) were of the same type while the third belonged to a different type. Again, in $[\text{Rh}_4(\text{CO})_{12}]$, the three Rh (0) were of one type and the fourth was of different type because the software gave two types of each of shielding constants and the magnetic terms in these two carbonyls respectively (Tables: 3-6). Same inference was drawn from the charges on metal ions where the spatially different metals possessed different charges (Table:8).
- (9) $[\text{Fe}_3(\text{CO})_{12}]$ contained five types of CO s with 5 sets of values of $\sigma^{13}\text{C}$, $\sigma^{17}\text{O}$ and $\delta^{13}\text{C}$, $\delta^{17}\text{O}$ respectively. Two bridging COs (Table: 10) possessing lowest set of values of $\sigma^{13}\text{C}$ and $\delta^{17}\text{O}$ (highest set of $\delta^{13}\text{C}$, $\delta^{17}\text{O}$) respectively were of the first type. Second type consisted of four terminal COs (Table-10) with another set of values of $\sigma^{13}\text{C}$, $\sigma^{17}\text{O}$ and $\delta^{13}\text{C}$, $\delta^{17}\text{O}$. Each one of the remaining three types of CO s (Table-10) contained two similar terminal COs with three different sets of $\sigma^{13}\text{C}$, $\sigma^{17}\text{O}$ and $\delta^{13}\text{C}$, $\delta^{17}\text{O}$ values respectively.
- (10) $[\text{Rh}_4(\text{CO})_{12}]$ contained four types of COs. Three bridging COs, though bonded to two different sets of Rh (0) showed lowest but same set of $\sigma^{13}\text{C}$ and $\sigma^{17}\text{O}$ (highest set of $\delta^{13}\text{C}$, $\delta^{17}\text{O}$) values and thus belonged to the same type (Table-10). Each one of the remaining three types of COs containing three similar terminal COs (Table-10) with three different sets of $\sigma^{13}\text{C}$, $\sigma^{17}\text{O}$, $\delta^{13}\text{C}$, $\delta^{17}\text{O}$ values belonged to three different types.

Structures and explanation of NMR parameters of $\text{M}_3(\text{CO})_{12}$ {M=Ru,Os}

Their formation, reasons for change in NMR parameters and large differences in $\sigma^{13}\text{C}$, $\sigma^{17}\text{O}$, $\delta^{13}\text{C}$, $\delta^{17}\text{O}$ values in these carbonyls, was explained as follows:

Table 9: Atomic Electron Valence Density (integrated)/ L Value and Charges on O

Carbonyl	ADF Numbers of O	$\sigma^{13}\text{C}$ (MCO)	AEVD (integrated)/ L Value at O* [Average AEVD /L/O]	Charge on O** [Average Charge/O]
$\text{Ru}_3(\text{CO})_{12}$ (1)	(5,7,17,19,23,25)	-192.8	6.384	-0.377
	(9,10,13,15,20,27)	-115.5	6.377	-0.384
			[6.381]	[-0.381]
$\text{Os}_3(\text{CO})_{12}$ (2)	(4,7,9,19,21,27)	-94.7	6.39	-0.39
	(11,13,15,17,22,25)	-155	6.385	-0.385
			[6.388]	[-0.388]
$\text{Ir}_4(\text{CO})_{12}$ (3)	(4,6,8,9,12,13,18, 19, 22,23,25,28)	-41.57	6.36	-0.36
			[6.360]	[-0.360]
$\text{Fe}_3(\text{CO})_{12}$ (4)	(5,7)	-468.88	6.36	-0.347
	(9,11)	-59.35	6.354	-0.351
	(13,15)	-117.54	6.355	-0.36
	(17,18,21,23)	-82.34	6.6	-0.355
	(24,27)	-38.23	6.474	-0.354
			[6.457]	[-0.354]
$\text{Rh}_4(\text{CO})_{12}$ (5s)	(6,10,28)	-48.23	6.3492	-0.349
	(7,20,22)	-49.4	6.356	-0.356
	(12,14,16)	-337.92	6.382	-0.382
	(18,24,26)	-57.92	6.357	-0.357
			[6.361]	[-0.361]

*AEVD (integrated)/ L value at O=6.359 and **Charge on O= - 0.359 in uncoordinated CO (g)

$\text{Os}_3(\text{CO})_{12}$ {Fig:2} and its lighter analogue $\text{Ru}_3(\text{CO})_{12}$ {Fig:1} possessed D_{3h} symmetry consisting of an equilateral triangle of Os (0) or Ru (0) respectively. Each metal was directly bonded to two more metals, two axial and two equatorial CO ligands in a six coordinate trigonal prism geometry having sp^3d^2 hybridization²⁷. The d orbitals involved in this hybridization were: nd_xz , nd_{yz} { $n=4,5$; $M=\text{Ru, Os}$ } with major lobes pointing towards the vertices though not as directly as in the case of an octahedron. In the excited state, these two d orbitals on each metal being half filled would take part in

forming bonds with each one of the other two metals with their respective half filled orbitals. Each one of the remaining four vacant hybrid orbitals received a lone pair of electrons from the carbon of each one of four COs to form sigma bonds. The two axial COs attached to each metal being \wedge , did not back accept electron cloud from the filled nd_{xy} , $nd_{x^2-y^2}$, nd_{z^2} { $n=4,5$; $M=\text{Ru, Os}$ }. Rather, they would lose electron density. The Π^* molecular orbitals of carbon of two equatorial COs were geometrically favorable and energetically suitable with the above named filled orbitals of metal to back accept electron

Table 10: ADF Numbers and $\sigma^{13}\text{C}$ of C atoms a Bonded to Metals

Carbonyl [M Nos]	Spatially Equivalent C atoms with $\sigma^{13}\text{C}$	C bonded to 1 st metal	C bonded to 2 nd metal	C bonded to 3 rd metal	C bonded to 4 th metal
$\text{Ru}_3(\text{CO})_{12}$ [1,2,3]	C (4,6,16,18,22,24) = -67.23; T-1	(16,18) T-1	(22,24) T-1	(4,6) T-1	----
	C (8,11,12,14,21,26) = -31.2; T-2	(11,12) T-2	(14,26) T-2	(8,21) T-2	----
$\text{Os}_3(\text{CO})_{12}$ [1,2,3]	C(5,6,8,18,20,26) = -23.6; T-1	(6,8) T-1	(18,26) T-1	(5,20) T-1	----
	C(10,12,14,16,23,24) = -53.9; T-2	(10,12) T-2	(14,16) T-2	(23,24) T-2	----
$\text{Ir}_4(\text{CO})_{12}$ [1,2,3, 16]	C(5,7,10,11,14,15,17,20,21,24,26,27) = -5.41; T	(5,7,20) T	(10,14,27) T	(11,15,26) T	(17,21,24) T
$\text{Fe}_3(\text{CO})_{12}$ $\text{Fe}^6(1)$	C(4,6) = -120.66; B	(8,10,12,14) T-3,4	---	---	----
$\text{Fe}^6(1)$	C(8,10) = -13.01; T-3	----	(4,6) B	(4,6) B	----
$\text{Fe}^7(2,3)$	C(12,14) = -39.11; T-4	----	(19,22) T-1	(16,20) T-1	----
	C(16,19,20,22) = -24.0; T-1 C(25,26) = -1.89; T-2	----	(26) T-2	(25) T-2	----
$\text{Rh}_4(\text{CO})_{12}$	C(5,9,27) = 2.81 ; T-3	(13) B	----	----	(13) B
$\text{Rh}^7(1,2,4)$	C(8,19,21) = -0.55 ; T-1	----	(11) B	----	(11) B
$\text{Rh}^6(3)$	C(11,13,15) = -77.52; B	(15) B	(15) B	----	----
	C(17,23,25) = -4.99; T-2	(21) T-1 (23) T-2 ----	(19) T-1 (17) T-2 ----	----	(8) T-1 (25) T-2 ----
				(5,9,27) T-3	---

a. ADF Numbers in parentheses [Figs: 1-5] ; T,T-1,T-2,T-3-terminal, B-bridging

Table 11: Spatial Classification of Metals & CO Groups

Carbonyl	Types of σM	Types of $\sigma^{13}\text{C}$ & $\sigma^{17}\text{O}$	No of spatially different M & CO Ligands
$\text{Ru}_3(\text{CO})_{12}$	One	Two each	Metals of same type; 2 types of COs; each having 6 COs
$\text{Os}_3(\text{CO})_{12}$	-do-	-do-	-do-
$\text{Ir}_4(\text{CO})_{12}$	-do-	One each	All Ir of same type; all 12 COs of same type
$\text{Fe}_3(\text{CO})_{12}$	Two	Five each	2 types of Fe; 2 of 1st type and one of 2nd type; 5 types of COs; 2 each of 4 types & 4 of 5th type
$\text{Rh}_4(\text{CO})_{12}$	Two	Four each	Two types of Rh; 3 of 1st & one of 2nd type; 4 types of Co; each having 3 CO

Table 12: k, j & H^{spin} Values of Nuclei in Poly-nuclear Carbonyls

Perturbing nucleus ^a (Fig. No.)	Responding nuclei ^a	k [10^{19} kg m ⁻² s ⁻² A ⁻²]	j (p pm)		H ^{spin} ($_{10}^{17}$ MHz mol ⁻¹)
* Ru₃(CO)₁₂					
Ru(1*) (1)	Ru(2)	626.377	0		
	Ru(3)	631.106	0		
	C(4,6)	-35.569	0		
	C(8)	-15.592	0		
	C(11,12)	678.35	0		*
	C(14)	-16.743	0		
	C(16,18)	1012.29	0		
	C(21,26)	93.405	0		
Ru(2)* (1)	C(22,24)	-34.694	0		
	Ru(1)	626.377	0		
	Ru(3)	631.106	0		
	C(4,6)	-35.569	0		
	C(8,11)	93.405	0		
	C(12)	-16.743	0		
	C(14,26)	677.722	0		*
	C(16,18)	-34.694	0.000	0.000	
Ru(3)* (1)	C(21)	-15.592	0		
	C(22,24)	1012.29	0		
	Ru(1,2)	631.107	0		
	C(4,6)	1013.11	0		
	C(8,21)	677.741	0		
	C(11,26)	-16.173	0		
	C(12,14)	93.932	0		*
	C(16,18,22,24)	-35.011	0		
Os₃(CO)₁₂					
Os(1) (2)	Os(2,3)	-410.441	-2.648		-35.885
	C(5,18)	-45.45	-3.182		-14.374
	C(6,8)	635.726	44.511		201.067
	C(10,12)	707.485	49.535		223.762
	C(14,16,23,24)	-4.748	-0.332		-1.5
	C(20,26)	-2.366	-0.166		-0.75
Os(2) (2)	Os(1,3)	410.441	-2.648		-35.885
	C(5,8)	-2.366	-0.166		-0.75
	C(6,20)	-45.45	-3.182		-2.386
	C(10,12)	-4.748	-0.332		-1.5
	C(14,16,18,26)	707.485	49.535		223.762
Os(3) (2)	C(23,24)	635.726	44.511		201.067
	Os(2,3)	-410.441	-2.648		-35.885
	C(5,20)	635.778	44.511		201.067
	C(6,18)	-2.363	-3.182		-0.75

	C(8,26)	-45.45	-0.332	14.374
	C(10,12,14,16)	-4.748	-0.332	1.5
	C(23,24)	707.448	49.532	223.748
**Ir₄(CO)₁₂				
Ir(1)** (3)	Ir (2,3,16)	747.876	0	
	C(5,7,20)	659.731	0	**
	C(10,15,24)	11.794	0	
	C(11,14,17,21,26,27)	-5.654	0	
Ir(2)** (3)	Ir(1,3,16)	747.876	0	
	C(5,15,17,20,24,26)	-5.654	0	**
	C(7,11,21)	11.795	0	
	C(10,14,27)	659.729	0	
Ir(3)** (3)	Ir(1,2,16)	747.859	0	
	C(5,7,10,14,21,24)	-5.656	0	**
	C(11,15,26)	659.661	0	
	C(17,20,27)	11.801	0	
Ir (16)** (3)	Ir(1,2,3)	747.817	0	
	C(5,14,26)	11.786	0	**
	C(7,10,11,15,20,27)	-5.654	0	
	C(17,21,24)	659.787	0	
Fe₃(CO)₁₂				
Fe(1) (4)	Fe(2,3)	344.153	4.312	6.493
	C(4,6)	-40.367	-3.939	-5.931
	C(8,10)	502.096	48.989	73.765
	C(12,14)	581.249	56.712	85.394
	C(16,19,20,22)	-19.52	-1.905	-2.869
	C(25,26)	-41.822	-4.08	6.144
Fe(2) (4)	Fe(1)	344.152	4.312	6.493
	Fe(3)	628.242	7.871	11.852
	C(4,6)	408.772	39.884	60.055
	C(8)	-49.395	4.819	7.256
	C(10)	15.708	1.533	2.308
	C(12,14,25)	-26.383	-2.574	-3.876
	C(16,20)	-14.134	-1.379	-2.076
	C(19,22)	574.352	56.039	84.381
	C(26)	578.501	56.444	85.394
Fe(3) (4)	Fe(1)	344.152	4.312	6.493
	Fe(2)	628.242	7.871	11.852
	C(4,6)	408.772	39.884	60.055
	C(8)	15.707	1.533	2.308
	C(10)	-49.395	-4.819	-7.256
	C(12,14,26)	-26.383	-2.574	-3.876
	C(16,20)	574.352	56.039	84.381
	C(19,22)	-14.134	-1.379	-2.076
	C(25)	578.501	56.444	84.991

$\text{Rh}_4(\text{CO})_{12}$					
Rh(1) (5)	Rh(2,4)	1097.61	13.185	19.853	
	Rh(3)	663.282	7.968	11.998	
	C(5)	21.888	-2.091	-3.149	
	C(8,19)	-9.73	0.93	1.4	
	C(9,27)	-13.041	1.246	1.876	
	C(11)	103.312	-9.87	-14.862	
	C(13,15)	710.396	-67.869	-102.179	
	C(17,25)	93.874	-8.968	-13.504	
	C(21)	826.648	-78.976	-82.650	-118.918
	C(23)	865.109			-124.45
Rh(2) (5)	Rh(1,4)	1097.61	13.185	19.853	
	Rh(3)	663.284	7.968	11.998	
	C(5,9)	-13.125	1.254	1.888	
	C(8,21)	-9.733	0.93	1.4	
	C(11,15)	710.397	-67.869	-102.179	
	C(13)	103.312	-9.87	14.862	
	C(17)	865.109	-82.65	-124.45	
	C(19)	826.649	-87.944	-118.918	
	C(23,25)	93.874	-2.091	-13.504	
	C(27)	21.888			-3.149
Rh(3) (5)	Rh(1,2,4)	663.277	7.968	11.998	
	C(5,9,27)	725.205	-69.284	-104.324	
	C(8,19,21)	57.227	-5.467	-8.232	
	C(11,13,15)	102.109	-9.755	-14.689	
	C(17,23,25)	25.293	-2.416	-3.638	
Rh(4) (5)	Rh(1,2)	1097.71	13.186	19.854	
	Rh(3)	663.372	7.969	11.998	
	C(5,27)	-12.916	-1.234	-1.858	
	C(8)	826.254	-78.938	-118.86	
	C(9)	22.327	-2.133	-3.212	
	C(11,13)	710.361	-67.866	-102.178	
	C(15)	103	-9.885	-14.884	
	C(17,23)	93.767	-8.958	-13.489	
	C(19,21)	-9.802	0.936	1.409	
C(25)	864.835	-82.624	-124.411		

a. ADF Numbers in parentheses [Figs:1,2,3]; *No spin-spin interaction due to large difference in % abundance of ^{101}Ru (17.07%) and ^{13}C (1.1%) **Large difference in $\gamma^{191}\text{Ir}$ (0.509) and $\gamma^{13}\text{C}$ (6.7383)

cloud to increase the electron density. This caused the two equatorial COs to show an increase in $\sigma^{13}\text{C}$ and $\delta^{17}\text{O}$ values. As the decrease in electron density in two axial COs overweighed this increase by the two equatorial COs, the Total Coordination Shift was found to be negative (Tables: 7,14). The 6 axial(2 on each M) and the other 6 equatorial(2 on

each M) would make two types of terminal (T-1; T-2) COs (Table-10) in each one of the carbonyls.

Structure and explanation of observed NMR parameters in $\text{Ir}_4(\text{CO})_{12}$

$\text{Ir}_4(\text{CO})_{12}$ showed a regular T_d symmetry {Fig:3}; with each Ir(0) being six coordinate having

sp³d² hybridization. Three half filled hybrid orbitals of one Ir(0) overlapped with similar hybrid orbitals on each of the other three Ir(0) to form a regular tetrahedron whose each vertex was occupied by Ir (0). Each one of its remaining three vacant sp³d² hybrid orbitals would receive a lone pair of electrons from each one of the three carbon atoms of the COs

and back accept electron cloud from the three filled d orbitals of Ir (0) to form bonds with three equivalent terminals COs. The increase in electron density was indicated by the increased $\sigma^{13}\text{C}$ and $\sigma^{17}\text{O}$ values. The 12 terminal COs were found to be spatially equivalent (Table:10) having the same $\sigma^{13}\text{C}$ and $\sigma^{17}\text{O}$ values respectively.

Table 13: Designation of IR/Raman Bands and Their Vibration Symmetry Classes

Carbonyl	Vibration Symmetries of bands	IR-active bands	Raman-active bands	Both IR and Raman active bands	IR inactive bands	May not be Raman a, b observed bands	Vibration Symmetry Class
[M ₃ (CO) ₁₂] (M= Ru , Os)	A ₁	----	A ₁ (13)	----	A ₁ (13)	----	[13A ₁ +12A ₂ +25E]
[D ₃]	A ₂	A ₂ (12)	A ₂ ² (12)	A ₂ (12)	---	A ₂ a (1 ₂)	
[Ir ₄ (CO) ₁₂]	E	E(50)	E(50)	E(50)	----	----	
[T _d]	A ₁	-----	A ₁ (5)	-----	A ₁ (5)	A ₁ b (5)	[5A ₁ +2A ₂ +7E+8T ₁ +11T ₂]
	A ₂	-----	A ₂ (2)	-----	A ₂ (2)	A ₂ a (2)	
	E	-----	E(14)	-----	E(14)	---	
	T ₁	-----	T ₁ (24)	-----	T ₁ (24)	T ₁ ^a (24)	
	T ₂	T ₂ (33)	T ₂ (33)	T ₂ (33)	-----	----	
[Fe ₃ (CO) ₁₂]	A ₁	A ₁ (24)	A ₁ (24)	A ₁ (24)	---	---	[24A ₁ +14A ₂ +19B ₁ +18 B ₂]
[C _{2v}]	A ₂		---	A ₂ (14)	---	A ₂ (14)	- - -
	B ₁	B ₁ (19)	B ₁ (19)	B ₁ (19)	----	---	
	B ₂	B ₂ (18)	B ₂ (18)	B ₂ (18)	---	---	
[Rh ₄ (CO) ₁₂]	A ₁	A ₁ (18)	A ₁ (18)	A ₁ (18)		---	[18A ₁ +8A ₂ +26 E]
[C _{3v}]	A ₂	----	A ₂ (8)		A ₂ (8)	^a $\frac{1}{2}$	
	E		E (52)	E (52)	E (52)		---

*Numbers in parentheses indicate the bands of a specific symmetry. a. Raman active; but intensity being 10-29 to-30; were not observed. b. Raman active but Depolarization ratio (linear) ≈ 0 .0; were not observed

Table 14: Coordination Shifts of [M₃(CO)₁₂] (M= Ru, Os)

Carbonyl	IR bands (cm ⁻¹) {Raman bands (cm ⁻¹)}	Total Coordination Shift ($\Delta \delta^{13}\text{C}_T$) [Relation:6]	S _{M-M} (kJ mol ⁻¹)	d _{M-M} (Å ^o)
[Ru ₃ (CO) ₁₂][21]	2062 , 2026, 2002,1989 {2127,2034,2004,1994}	-177.3 = [(-67.23+34.44)*6 +(-31.2+34.44)*6]	78.0	2.85
[Os ₃ (CO) ₁₂][21]	2070 , 2019, 1998,1986 {2130,2028,2006,1989}	-51.9 = [(-53.9+34.44)*6 +(-23.63+34.44)*6]	94.0	2.88

Structure and explanation of observed NMR parameters in $[\text{Fe}_3(\text{CO})_{12}]$

Although, a variety in the spatial positions of CO groups made it cumbersome to assign reasons for very large difference in $\sigma^{13}\text{C}$, $\sigma^{17}\text{O}$, $\delta^{13}\text{C}$, $\delta^{17}\text{O}$ values in this carbonyls, yet the following points would make it easy to understand.

- (i) $[\text{Fe}_3(\text{CO})_{12}]$ {Fig:4;Table:10} contained two seven coordinate $\{\text{Fe}^7(0)\}$ and one six coordinate $\{\text{Fe}^6(0)\}$ iron with two bridging COs attached to both the $[\text{Fe}^7(0)]$. The remaining ten terminal Cos were attached to all the three Fe (0).
- (ii) In the six coordinate C_{2v} bicapped tetrahedron involving sp^3d^2 hybridization, two half filled d orbitals (dz^2 , d_{xz}) and four empty orbitals were involved. In addition, $\text{Fe}^6(0)$ possessed three filled atomic orbitals. Each one of the two half filled sp^3d^2 hybrid orbital of $\text{Fe}^6(0)$ overlapped with each one of the half filled sp^3d^3 hybrid orbital on each of the two $\text{Fe}^7(0)$ to form two $\text{Fe}^6\text{-Fe}^7$ bonds. There were now left four vacant sp^3d^2 hybrid orbitals on Fe (0). Each one would receive a lone pairs of electrons from the carbon atom of each one of four COs to form four bonds. Two axial COs being \wedge to the metal did not back accept the electron cloud from the filled $3d_{xy}$, $3d_{yz}$, $3d_{x^2-y^2}$ of this $\text{Fe}^6(0)$ because their symmetries were not compatible. Rather, they lost some electron density to make their $\sigma^{13}\text{C}$ and $\sigma^{17}\text{O}$ values less than reference values (T-3). The other two COs being equatorial, back accepted electron cloud from the filled d orbitals of $\text{Fe}^6(0)$ to make their $\sigma^{13}\text{C}$ and $\sigma^{17}\text{O}$ values more than reference values(T-4).
- (iii) Each one of the seven coordinate capped octahedron involving sp^3d^3 (d_z^2 , d_{xz} , d_{yz}) hybridization²⁷ possessed four half filled and three vacant hybrid orbitals. In addition, there were lying two filled atomic orbitals (d_{xy} , $d_{x^2-y^2}$) on $\text{Fe}^7(0)$. Three vacant sp^3d^3 hybrid orbitals on each one of the two $\text{Fe}^7(0)$ formed three bonds with the three COs. Each one of these COs would back accept the electron cloud from the filled d_{xy} orbital so that their $\sigma^{13}\text{C}$ and $\sigma^{17}\text{O}$ values became more than the reference values. Of course, in one CO where the geometries and energies

of the filled $3d_{xy}$ of $\text{Fe}^7(0)$ and Π^* of CO were compatible received back more electron cloud than the other two CO. This made two COs {one on each $\text{Fe}^7(0)$ } to have higher $\sigma^{13}\text{C}$ and $\sigma^{17}\text{O}$ values to act as terminal carbonyls (T-2) while the remaining four COs; two lying on each $\text{Fe}^7(0)$ which would act another set of four terminal carbonyls (T-1).

- (iv) Two of the four half filled hybrid orbitals were then used in forming two types of M-M bonds ($\text{Fe}^7\text{-Fe}^6$ and $\text{Fe}^7\text{-Fe}^7$) with two different bond energies (65.0, 52.0 kJ mol⁻¹) and different bond lengths {2.56, 2.68 (Å)}²⁸
- (v) This would leave two half filled hybrid orbitals on each $\text{Fe}^7(0)$ unparticipating. A total of these four half filled orbitals; {two on each of the two $\text{Fe}^7(0)$ } and the two sigma lone pairs (one on each CO), then, overlapped to form four sigma bonds with two bridging COs (B) with these two $\text{Fe}^7(0)$. As the bridging COs did not back accept electron cloud, their $\sigma^{13}\text{C}$ and $\sigma^{17}\text{O}$ values showed a decrease.

Thus this NMR study gave a fillip to Mossbauer studies (MS) of $\text{Fe}_3(\text{CO})_{12}$. It was MS which, first of all, confirmed its C_{2v} structure showing quadrupole doublets with similar isomer shifts but different quadrupolar coupling constants (1.13 and 0.13 (mms⁻¹)^{23,24}. The software also showed the C_{2v} point group structure for $\text{Fe}_3(\text{CO})_{12}$. The two $\text{Fe}^7(0)$ possessed the same values of important NMR parameters such as [σFe^7 and δFe^7 (Tables:4)]; total diamagnetic and paramagnetic contributions (Table:6); charges on Metal Ions (Table:8); values of k and j (Table:12)]. In addition, both the bridging CO groups which were bonded with the two Fe^7 showed the same values of their NMR parameters.

Structure and explanation of observed NMR parameters in $\text{Rh}_4(\text{CO})_{12}$

Again, the following points would make it easy to understand:

- (i) $\text{Rh}_4(\text{CO})_{12}$ showed C_{3v} symmetry {Fig:5;Table:10}. Each metal was directly bonded to three more metals, i. e. there was an array of four Rh (0) with nine terminal COs and three bridging COs. Only one Rh (0) was six coordinate $\{\text{Rh}^6(0)\}$ which was

bonded to the remaining three Rh (0); each having coordination number seven (Rh⁷ (0)) to form three Rh⁶-Rh⁷ bonds. In addition, the {Rh⁶ (0)} was further bonded to three terminal COs. On the other hand, each one of the three Rh⁷ (0) was directly bonded three Rh (0) {one Rh⁶ (0) and two Rh⁷ (0)}, two terminal COs and two bridging COs as explained below:

- (ii) Rh⁶ (0) with sp³d² hybridization possessed three half filled hybrid orbitals and three vacant hybrid orbitals. In addition, Rh⁶(0) possessed three completely filled atomic orbitals. Each one of the three half filled sp³d² hybrid orbitals formed three Rh⁶ – Rh⁷ bonds with each one of the three other Rh⁷(0) by overlapping with each one of their half filled sp³d³ hybrid orbital respectively.
- (iii) Each one of the remaining three vacant sp³d² hybrid orbitals received a lone pair of electrons from carbon atom of each one of the three COs. These three COs, then, back accepted electron cloud from the three filled d orbitals of Rh⁶ (0) to increase the electron density which was confirmed by their increased $\sigma^{13}\text{C}$ and $\sigma^{17}\text{O}$ values. Thus the three COs acted as the terminal groups (T-3) with Rh⁶ (0).
- (iv) Now each one of the three Rh⁷ (0) with sp³ d³ hybridization (having three half filled hybrid orbitals and four vacant hybrid orbitals) with two completely filled atomic orbitals was left with two half filled and two vacant sp³ d³ hybrid orbitals after forming a Rh⁶-Rh⁷ bond. Each one of the two half filled hybrid orbitals on each Rh⁷ (0) formed two Rh⁷-Rh⁷ bonds with each of the two similar Rh⁷ (0).
- (v) Then, each one of the other two vacant hybrid orbitals received the lone pair from carbon of CO; back accepted the electron cloud from two filled atomic orbitals to increase the electron density as indicated by the increased $\sigma^{13}\text{C}$ and $\sigma^{17}\text{O}$ values. The two terminal COs on each one of these three Rh⁷(0) were of two types spatially (one axial and other[^]). So, the 9 terminal COs were of three types. Six COs bonded to three Rh⁷ (0) were divided into two types of terminal COs (T-1, T-2); one T-1 and one T-2 were bonded to each one of the three Rh⁷ (0)}. As already explained, three terminal COs (T-3) were bonded to Rh⁶ (0).
- (vi) There were still left six half filled atomic

orbitals {two on each one of the three Rh⁷(0)} and three lone pairs of electrons on three COs which acted as bridging COs with these three Rh⁷(0) involving two Rh⁷(0) at a time. Thus, each one of three Rh⁷(0) was bonded to two bridging COs. Various spatial displacements of COs having different shielding constants were given in (Tables:10,11).

Spatial and Magnetic Equivalence of metals and CO groups

- (a) In none of these poly-nuclear carbonyls, the metals or any two COs were both spatially and magnetically equivalent i.e. did not have same σ , δ , k and j values with other nuclei of the molecule in addition to having same values among themselves.
- (b) The four Ir(0) and 12 COs were stereochemically equivalent respectively.
- (c) The various spatial displacements observed for the twelve COs having different shielding constants were given in (Tables:10,11).

Calculation of Effective Spin Hamiltonian (H^{Spin}) of M and ¹³C nuclei

Spin-spin coupling parameter (j) was related to another important NMR called Effective Spin Hamiltonian (H^{Spin}) which represented a mathematical expression to determine the energy of an NMR transition in a molecule. The word "effective" implied that its solutions reproduce the nuclear magnetic energy levels in a molecular system without reference to electrons. In a fictitious absence of surrounding electrons, the shielding constants and indirect spin-spin coupling constants would vanish leaving the NMR spectrum to be determined by Nuclear Zeeman Term and direct dipolar coupling. A simple relation to calculate Effective Spin Hamiltonian (H^{Spin}) values of the metals and the bonded carbon atoms from their j [p pm] values as given by relation (7) and stated in²⁵ (Table:12)

$$H^{\text{Spin}} = 6.023 j \text{ A B. IA. . IB. MHz mol}^{-1} \dots(7)$$

Classification of (3n-6) fundamental vibration bands into their IR and Raman activities and the Vibration Symmetry Classes

Both IR and Raman spectra of the five poly-nuclear carbonyls were studied with their Vibration Symmetry Classes. A definite vibration

symmetry symbol was given to each one of their (3n-6) fundamental vibration bands. The bands were classified as IR-active, Raman-active and both IR- and Raman-active. Some Raman-active bands which possessed negligibly small intensities or had depolarization ratios ≈ 0 were not observed in the spectra (Table:13). Unlike their experimental determination²⁹⁻³², here the Raman intensities were calculated from the polarizabilities³³⁻³⁷ and, thus, were expected to have exact values. The discussion regarding IR/Raman was divided into four parts:

- (i) The 75 bands in each of $M_3(CO)_{12}$ (M= Ru,Os) were classified into symmetry symbols A_1, A_2 and E having 13, 12 and 50 bands respectively. So their Vibration Symmetry Class was shown as: $\{13A_1+12A_2+25E\}$ (Table:13; A_1, A_2 being singly and E being doubly degenerate).
- (ii) 78 bands in $Ir_4(CO)_{12}$ were classified into symmetry symbols A_1, A_2, E, T_1 and T_2 , having 5, 2, 14, 24 and 33 bands respectively with Vibration Symmetry Class as: $\{5A_1+2A_2+7E+8T_1+11T_2\}$ (Table:13; T_1, T_2 being triply degenerate).
- (iii) 75 bands in each of $Fe_3(CO)_{12}$ were classified into symmetry symbols A_1, A_2, B_1 and B_2 having 24, 14, 19 and 18 bands respectively with Vibration Symmetry Class as: $\{24A_1+14A_2+19B_1+18B_2\}$ (Table:13; B_1, B_2 being triply degenerate).
- (iv) The 78 bands in $Rh_4(CO)_{12}$ were classified into symmetry symbols A_1, A_2 and E having 8, 18, and 52 bands respectively with Vibration Symmetry Class as: $\{18A_1+8A_2+26E\}$ (Table:13).

Confirmation of Π -back acceptor character of carbonyls from NMR

This NMR study confirmed the Π -back-acceptor nature of carbonyls in two ways:

Corroboration between total coordination shift ($\Delta \delta C_T$) and $[v_{CO}]$ values

Since, the carbonyls possessed stereo chemically different CO groups with different δC values, it would be better to correlate their $[v_{CO}]$ values with their Total Coordination Shift ($\Delta \delta C_T$) values which were the averaged values of δC for

all the carbonyl groups in any metal carbonyl. Depending upon the similarities in their symmetries, the discussion was divided into three headings as follows:

$M_3(CO)_{12}$ {M=Ru, Os}

As the Total Coordination Shift ($\Delta \delta C_T$) increased, the nCO (cm^{-1}) also increased to decrease the Π -back accepting capacity of electron cloud by the metals. The NMR studies corroborated well with IR studies because like νCO , the ($\Delta \delta^{13}C_T$) values^{38,39} were also found to be higher in $Os_3(CO)_{12}$ than $Ru_3(CO)_{12}$ as both possessed the same symmetry point group (D_{3h}) (Table:14).

$Ir_4(CO)_{12}$

Since all the 12 carbonyl groups of $Ir(0)$ were found to be stereo chemically equivalent; each having higher $\sigma^{13}C$ and $\sigma^{17}O$ values (5.41 and -41.57 ppm) than the reference values (-34.44 and -129.53 ppm) and thus confirmed the higher electron density on carbon of each carbonyl group than that on $CO(g)$ to prove the back accepting nature of $Ir_4(CO)_{12}$ with T_d symmetry (Tables:4,5).

$Fe_3(CO)_{12}$ and $M_4(CO)_{12}$

With different point group symmetries (C_{2v}, C_{3v}) and different number of bridging and terminal carbonyl groups, no comparison was possible in their Total Coordination Shift ($\Delta \delta C_T$).

But, their Π -back acceptor character was confirmed by (B) as follows:

From the Charges and AEVD Values on ^{17}O and Metals

This NMR study proved two facts simultaneously:

Acceptance of electron density by CO groups

Since ^{17}O became more negative (though small) than ^{17}O of $CO(g)$ to show higher AEVD {Atomic Electron Valence Density (integrated)/L} than ^{17}O of $CO(g)$ (Table:9) to confirm the acceptance of electron cloud from the metal/s.

Back donation of electron cloud by the metals

Again, each metal acquired a very small positive charge (Table:8) to prove that the metal/s would donate electron density to CO groups.

Hence like vibration spectral studies, the NMR studies also confirmed the synergic nature of the metal carbonyls.

CONCLUSION

We are able to reaffirm the relative spatial displacements of both the terminal and bridging carbonyl groups and the π -acid character of the carbonyls from the NMR parameters of ^{13}C and ^{17}O nuclei such as $\sigma^{13}\text{C}$, $\sigma^{17}\text{O}$, $\delta^{13}\text{C}$, $\delta^{17}\text{O}$ along with the

six diamagnetic and paramagnetic constituting terms of σM , $\sigma^{13}\text{C}$ and $\sigma^{17}\text{O}$. We were also able to confirm the spatial equivalence/nonequivalence of the three/four metal ions of the carbonyls. This NMR studies corroborated with the results already obtained from their IR/Raman studies. Lastly, we could identify some bands which, no doubt, were Raman active but because of their negligible Raman intensities or linear Depolarization ratios could not be observed in their Raman spectra.

REFERENCES

- Sharma, S.; Chander, S.; Sehgal, M.L.; Ahmad, I. *Orient. J. Chem.* 2015, 31, 1417-27.
- Schreckenbach, G.; Ziegler, T. *J. Phys. Chem.* 1995, 99, 606-11.
- Schreckenbach, G.; Ziegler, T. *Int. J. Quantum Chem.* 1997, 61, 899-918.
- Sehgal, M.L.; Aggarwal, A.; Singh, S. *J. App. Chem.* 2016, 9, 48-64.
- Li, J.; Schreckenbach, G.; Ziegler, T. *J. Am. Chem. Soc.* 1995, 117, 486-94.
- Li, J.; Schreckenbach, G.; Ziegler, T. *J. Phys. Chem.* 1994, 98, 4838-41.
- Li, J.; Schreckenbach, G.; Ziegler, T. *Inorg. Chem.* 1995, 34, 3245-52.
- Nicholas, J. H.; Levason, W.; Webster, M. *J. Organomet. Chem.* 1998, 568, 213-23.
- Ruixue, J.; Wang, C.; Qiong, L.; Li, Q. S.; Xie, Y.; Bruce King, R.; Schaefer, H. F. *Australian J. Chem.* 2014, 67, 1318-23.
- Yi, Z.; Wang, S.; Feng, H.; Xie, Y.; Bruce King, R. *Int. J. Mol. Sci.* 2011, 12, 2216-31.
- Xu, B.; Li, Q.S.; Xie, Y.; Bruce King, R.; Schaefer, H.F. *Croat. Chem. Acta* 2009, 82, 207-18.
- Sizova, O.V.; Varshavskii, Y.S.; Nikolskii, A.B. *Russian J. Coordinat. Chem.* 2005, 31, 875-83.
- Qiong, L.; Li, Q.S. *Chem. J. Chinese Universities* 2008, 29, 2430-34.
- Feng, X.; Gu, J.; Xie, Y.; Schaefer, H.F. *J. Chem. Theory and Comput.* 2007, 3, 1580-87.
- Ishikawa, Y.; Hackett, P. A.; Rayner, D. M. *J. Am. Chem. Soc.* 1987, 109, 6644.
- Tang, L.; Qiong, L.; Li, Q.S.; Xie, Y.; Bruce King, R.; Schaefer, H.F. *J. Chem. Theory Comput.* 2011, 7, 2112-25.
- Liu, Z.; Li, Q.S.; Xie, Y.; Bruce King, R.; Schaefer, H.F. *Inorg. Chem.* 2007, 46, 1803-16.
- Forson, A.; Johnson, B.F.G.; Lewis, J.; Matheson, T. W.; Robinson, B. H.; Jackson, W.G. *J. Chem. Soc. Chem. Commun.* 1974, 1042-44.
- Iwai, K.; Katada, M.; Sano, H.; Iwasawa, Y. *J. Radioanalyt. Nuc. Chem.* 2005, 103.
- Shariff, E. K.; Raha, A. K.; Hassan, M.R.; Nicholson, B. K.; Rosenberg, E.; Sharmin, A.; Salassac, L. *Dalton Trans.* 2008, 32, 4212-19.
- Fang, F. Ph.D. Thesis, University of South Carolina 2012.
- Kan, Y. Ph.D. Thesis, University of South Carolina 2013.
- Cotton, F. A.; Hunter, D. L. *Inorg. Chem. Acta* 1974, 11, L9.
- Cristopher, G.; Benson, G.; Long, G.; Kolis, J.W.; Shriver, D.F. *J. Am. Chem. Soc.* 1985, 107, 5297-98.
- Autschbach, J. *Str. Bond.* 2004, 112, 1-43.
- Nakamoto, K. 4th Edn.; Wiley- Interscience publication, N.Y. 1986, 291-98.
- Bruce King, R. *Coordinat. Chem. Rev.* 2004, 197, 141-68.
- Braga, D.; Farrugia, L.; Grepioni, F.; Johnson,

- B.F.J. *J. Org. Chem.* 1994, 464, C39-C41.
29. Chabal, Y.J.; Rayon, P.R. *J. Mol. Spectrosc.* 1962, 8, 164.
30. Schrotor, S.; Bernstein, H. J. *J. Mol. Spectrosc.* 1964, 12, 1.
31. Hartley, F. R.; Tunicliff, D.D.; Jones, A. A. *Spectrochem. Acta.* 1962, 18, 579.
32. Long, D.A.; Gravenor, R.B.; Milner, D.C. *Trans. Faraday Soc.* 1963, 59, 46-52.
33. Van Gisbergen, S.J. A.; Snijders, R. J. G.; Baerends, E. J. *J. Chem. Phys.* 1995, 103, 9347.
34. Van Gisbergen, S.J.A.; Osinga, V.P.; Gritsenko, O.V.; Leeuwen, R.V.; Snijders, R.J.G.; Baerends, E. J. *J. Chem. Phys.* 1996, 105, 3142.
35. Van Gisbergen, S.J. A.; Snijders, R. J. G.; Baerends, E. J. *Chem. Phys. Lett.* 1996, 259, 599-604.
36. Osinga, V.P.; Van Gisbergen, S.J. A.; Snijders, R. J. G.; Baerends, E. J. *J. Chem. Phys.* 1997, 106, 5091-98.
37. Van Gisbergen, S.J. A.; Kootstra, F.; Schipper, P. R. T.; Gritsenko, O. V.; Snijders, J. G.; Baerends, E. J.; *Phys. Rev. A.* 1998, 57, 2556.
38. Quicksal, C. O. I and Spiro, T.G(1968)., *Inorg. Chem.*, 7:2365".
39. Kishner, S.; Fitzpatrick P.J.; Plowman K. R.; Butler, I. S. *J. Mol. Spectrosc.* 1981, 74, 29-37.